

Wavelet Transform Based Arterial Blood Pressure Waveform Delineator

Awadhesh Pachauri and Manabendra Bhuyan

Abstract— The proposed algorithm describes a novel wavelet transform based technique for extracting the features of arterial blood pressure (ABP) waveform. ABP waveform is rich in pathological information such as heart rate, systolic, mean and diastolic pressure thereby achieved an important aspect in cardiology. The multi-scale feature of wavelet transform enables systolic peaks to be detected from noise, base line drift, artifacts, irregular pressure waveform and arrhythmias. The first step in extracting ABP features starts from accurate detection of systolic peaks from ABP waveform. The algorithm is developed on the signals from MGH/MF waveform database, fantasia database, MIT-BIH Polysomnographic database and CSL database. The wavelets used for waveform delineation are symmetric (sym4) and Daubechies (db4). The technique involves decomposition of ABP signal up to nine levels by selected wavelet. The algorithm does not require any preprocessing before implementing the detection process. Relevant detail coefficient is selected based on energy, frequency and cross-correlation analysis of detail coefficients at each scale. Finally, selected detail coefficients undergo window based amplitude and interval thresholding for valid maxima detection termed as systolic peaks. Further, average coefficient obtained at first level is utilized for extracting other features such as onsets, diastolic notches and diastolic peaks taking systolic peaks positions as reference.

Keywords—Arterial blood pressure signal, wavelet transform, window based thresholding

I. INTRODUCTION

BLOOD pressure is the primary indicator of the health of the cardiovascular system of the body. ABP waveform depicts the cardiac function of contraction and relaxation. The systolic pressure indicates the contraction activity of heart whereas diastolic pressure specifies the relaxation behaviour of heart. ABP waveform comprises of systolic peak, diastolic onset, diastolic notch and a second smaller peak termed as diastolic peak. The appearance of diastolic notch in ABP waveform is due to closing of aortic valve. Diastolic peak in ABP waveform is the reflected impulse arising due to closing of aortic valve. Like electrocardiogram (ECG), ABP waveform is also rich in pathological information about cardiovascular

function. Blood pressure waveform analysis has been well recognized in cardiac physiology for the assessment of properties of arterial vessel wall [1], cardiac output monitoring [2], estimation of pressure pulse index [3] and cardiac arrhythmia detection [4]. Thereby it is well assumed that analysis of arterial blood pressure waveform can provide better insight of heart in cardiac physiology. Moreover, mathematical modeling of non-invasive ABP waveform has been used to estimate various cardiac parameters such as cardiac output, arterial compliance and peripheral resistance [5-8]. In certain conditions ECG signals may be excessively noisy or ECG acquisition may not be possible due to surgical dressing of patients. The noise on pressure signal is mechanical in nature whereas electrical noise interferes more in ECG. Therefore, analysis of ABP waveform can be used to estimate the cardiac health at certain stage when ECG waveform is not available. In some cases, parallel analysis of ABP waveform along with ECG has resulted in reducing false alarms to a certain extent for critical arrhythmias detection [9]. Ramaswamy et al [4] suggested that combination of ABP waveform along with ECG signal gave better results for the detection of ectopic beats than ECG signals only. Most of the algorithms on ABP signal are developed on proprietary datasets from selected patients and lack the robustness of modern ECG algorithms. Most of the algorithms require preprocessing and decision logic to detect the peaks. These methods are based on continuous independent assessment of refractory period (RP), analysis of signal by means of producing two moving averages [10], template matching [11], rank filter and decision logic [12], windowed and weighted Slope Sum Function (SSF) [13], peak and trough detection methods [4], heart rate, amplitude and interbeat intervals [14] and combinatorial analysis of ABP waveforms and their derivatives [15].

Algorithm developed by M. Aboy [14] includes peak detection of two ABP signals from CSL database. The algorithm utilizes a filter bank with variable cutoff frequencies, spectral estimates of the heart rate, rank-order nonlinear filters, and decision logic. The algorithm developed by Navakatikyan et al [10] is based on the continuous independent assessment of the refractory period (RP). Li et al [15] proposed an automatic delineator for the detection of fiducial points of arterial blood pressure waveforms, namely their onsets, systolic peaks and diastolic notches. It firstly seeks the pairs of inflection and zero-crossing points, and then utilizes combinatorial amplitude and interval criteria to select the onset and systolic peak. The

Awadhesh Pachauri is working towards PhD degree in department of electronics and communication engineering, Tezpur (central) university, Assam, India. (Phone: 91-7814480371, e-mail: awadhesh.pachauri @ gmail.com).

Manabendra Bhuyan is with department of electronics and communication engineering, Tezpur (central) university India and presently he is the dean, school of engineering. (e-mail: manab@tezu.ernet.in).

delineator is based on the combinatorial analysis of arterial blood pressure waveforms and their derivatives.

The researchers have paid major attention on the either systolic peaks [14], the onsets [11, 13], or diastolic notches only [16]. There are only few algorithms dedicated to the full characterization of ABP waveforms but these algorithms are limited to the detection of systolic peak, onsets and diastolic notch only and diastolic peak is not included [15]. However, detection of all four similar components has been shown by M Aboy et al on ICP signals [12]. Secondly, most of the developed algorithms merely accounted for physiological diversities [14]. Most of the recorded ABP signals suffer from instrumental unreliability and measuring inconsistency. In the third aspect, their validation and performance evaluation is based on their proprietary datasets. In particular, it is difficult to evaluate those systems and algorithms by their proprietary datasets [11, 16]. It is therefore essential to develop an algorithm that includes full characterization of ABP waveform, developed on open databases, includes performance, generality and robust against physiological interferences.

We suggest a wavelet transform based technique for full characterization of ABP waveform that is robust to physiological interferences and varying signal amplitude, does not require any preprocessing of signals, developed and validated on open access MGH/MF waveform database [17], Fantasia database [18], MIT-BIH polysomnographic database [19] and CSL database [20]. Moreover selection of detail coefficient after wavelet decomposition has been justified by energy, frequency and cross-correlation analysis of detail coefficients. Further application of window based threshold overcomes the problem of peaks missing due to large amplitude variations in the signal at any particular instant. The developed algorithm is applicable to any signal length however implementation of the algorithm is shown on first minute segment of Fantasia database, polysomnographic database and selected segment of MGH/MF database and CSL database for validation purpose.

II. MATERIALS

A. Discrete Wavelet Transform

Wavelets have been used for the illustration and analysis of many physiologic signals such as ECG and ABP signals because of their compact support. These physiologic signals can be reasonably characterized as isolated pulses or as sequences of pulses. Wavelet transform of a signal results in the concentration of signal energy in a relatively small number of coefficients that makes wavelet-based techniques potentially powerful tool for signal processing algorithms [21]. Noise generally encountered in the clinical environment is automatically eliminated due to inherent characteristics of wavelet technique.

A dyadic wavelet transform is implemented using the set of highpass and lowpass filters that are derived from coefficient wavelet referred as mother wavelet. These filters are called analytical filters. Detail signal and average signal are the outputs of highpass and lowpass filters respectively. These generated signals consist of small scale and bigger scale

information of the original signal. The lowpass filter coefficient undergoes subsampling to generate another new detail signal and average signal. Thus the dyadic discrete wavelet transform is the composition of dilated and translated form of mother wavelet. This process of decomposition of the signal may be continued until the average signal reaches the length of a single sample or a length that is not applicable for further application of the analysis filter pair [22].

The wavelet transform of a signal $x(t)$ is given by

$$W_a x(b) = \frac{1}{\sqrt{a}} \int_{-\infty}^{\infty} x(t) \psi\left(\frac{t-b}{a}\right) dt \quad (i)$$

Where $\psi((t-b)/a)$ is the shifted and scaled version of mother wavelet which is used as a basis for wavelet decomposition of the input signal. If the wavelet $\psi(t)$ is the derivative of a smoothing function $\theta(t)$, it can be shown that the wavelet transform of a signal $x(t)$ at a scale a is

$$W_a x(b) = -a \frac{d}{db} \int_{-\infty}^{\infty} x(t) \theta_a(t-b) dt \quad (ii)$$

Where $\theta_a(t-b) = \frac{1}{\sqrt{a}} \theta\left(\frac{t}{a}\right)$ is the scaled version of the smoothing function [23]. It is evident from the above equation that the wavelet transform at scale 'a' is proportional to the derivative of the filtered signal with a smoothing impulse response at scale 'a'. Hence zero crossings of wavelet transform at different scales will result in local maxima or minima and maximum slopes in the filtered signal will occur at maximum absolute values of wavelet transform [24].

Every decomposition results in decreasing the time resolution by a factor of 2 whereas the frequency resolution is doubled. Perfect reconstruction of the signal is possible only with the ideal half band filters such as Daubechies set of wavelets. For reconstruction purpose, the decomposition process is followed in reverse order. The wavelet coefficients obtained at each level are upsampled by two, and passed through synthesis filters (high pass and low pass) and are added. The analysis and synthesis filters are identical to each other, except for a time reversal. Therefore, the signal reconstruction is referred as the inverse DWT [25].

B. Validation Database

The ABP signals required for the analysis are acquired from openly available MGH/MF waveform database [17], Fantasia database [18], MIT-BIH polysomnographic database [19] and CSL database [20]. MGH/MF waveform database is the collection of recordings from 250 patients. The signals in the database are sampled at 360 samples/second. Each record consists of .dat file, .hea file and .ari file. Header file consists of information regarding the types of signals and type of leads in case of ECG signal, sampling interval, sampling frequency, duration of the signal and units. It comprises of the information to convert the recorded signals from raw units to physical units. The ari file consists of ECG annotations whereas dat file comprise of 8 signals.

Details of the record mgh007 of MGH database are given in table I. The segments of ABP signal when both ECG and ABP signals are available are considered for the analysis.

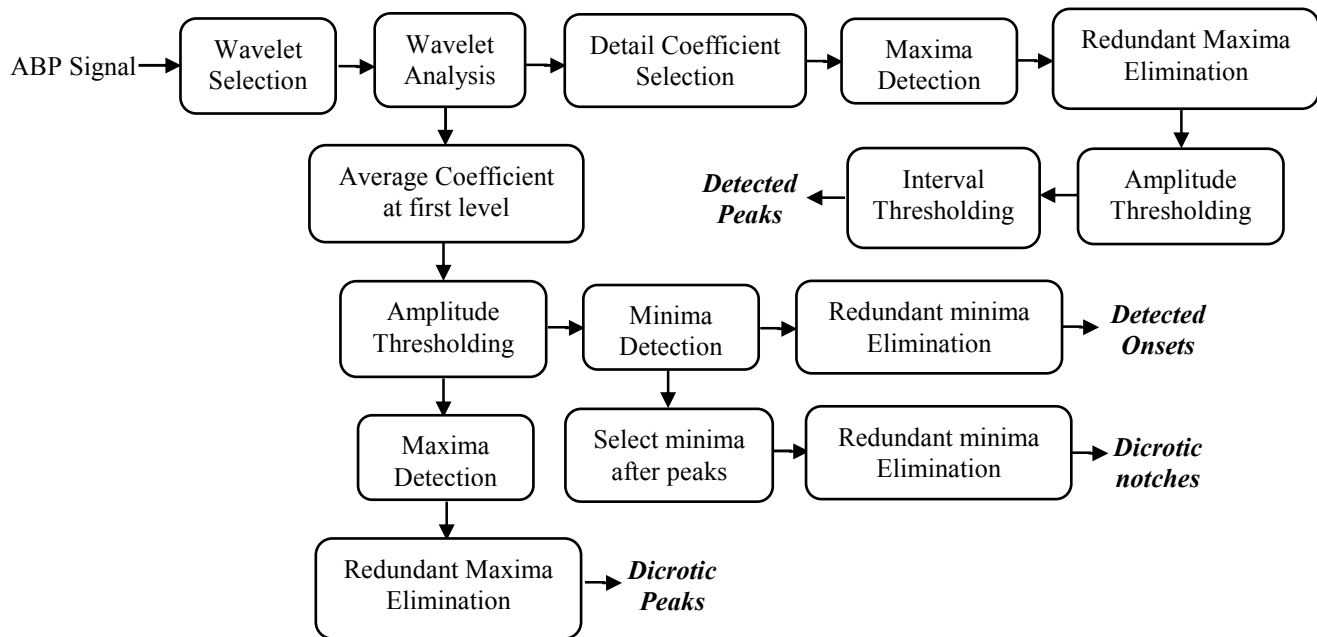


Fig 1. Block Diagram of Peak Detection Algorithm

TABLE I. DESCRIPTION OF RECORD MGH007 OF MGH/MF WAVEFORM DATABASE

Record	Signal	Gain	Base	Units
Mgh007	ECG lead I	1341	242	mV
	ECG lead II	1382	-618	mV
	ECG lead V	1295	-452	mV
	ABP	12.17	-1218	mmHg
	PAP	19.26	-1016	mmHg
	CVP	19.04	-1007	mmHg
	Resp. Imp.	1000	0	mV
	CO ₂	1000	0	mV

Fantasia and MIT-BIH polysmographic database signals are available on physionet. Both these database have ABP signal along with synchronously sampled ECG recordings. Signals in both the database are sampled at 250 Hz.

CSL database consists of two signals - abp1 and abp2 with approved annotations [20]. The available blood pressure signals are acquired from Pediatric Intensive Care Unit (PICU) at Deornbecher's Children's Hospital, Oregon Health and Science University. Signal acquisition was done by the data acquisition systems of Complex Systems Laboratory. The signals are sampled at 125 Hz. Manual annotation of both the records was performed by one expert by dividing each record in to non-overlapping segments each of one minute duration. The expert visually classified each segment as 'normal', corrupted or absent based on instructions for classifying segments proposed by Advancement of Medical Instrumentation (AAMI) [26].

III. DETECTION PROCEDURE

The signals from CSL database are readable by Matlab directly whereas the signals from MGH/MF waveform database, Fantasia and polysmographic database are not readable. These signals are converted into .mat files before

implementing the algorithm. In MGH/MF database, the extracted .mat file comprises of 8 signals as mentioned in table 1. The extracted signals are then separated to read each signal individually. Then the signals are converted from raw units to physical units. Finally, the samples of ABP and ECG II for the duration when both signals are available are considered for analysis. The detection process is performed on ABP signal of record mgh007 of MGH/MF database and abp1 signal of CSL database and completed in the following steps.

A. Peak Detection

ABP signal under test undergoes wavelet analysis by the selected wavelet. The relevant detail coefficients are selected from wavelet decomposition structure for maxima detection. The selected relevant maxima undergoes window based amplitude thresholding and interval thresholding to detect the ABP peaks. The block diagram of peak detection algorithm is shown in figure 1.

a) Wavelet Selection

There is no universal method suggested for selecting a particular wavelet. The choice of wavelet depends upon type of application. Generally, a wavelet similar in shape to the signal being analyzed is considered suitable for the

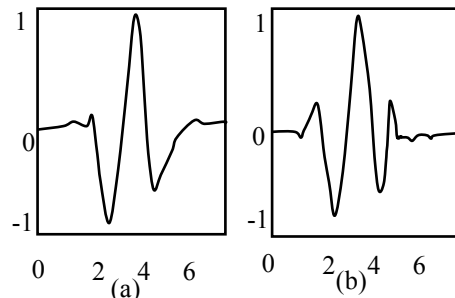


Fig2. Wavelet function (ψ) of (a) symmetric (sym4) wavelet and (b) daubechies (db4) wavelet

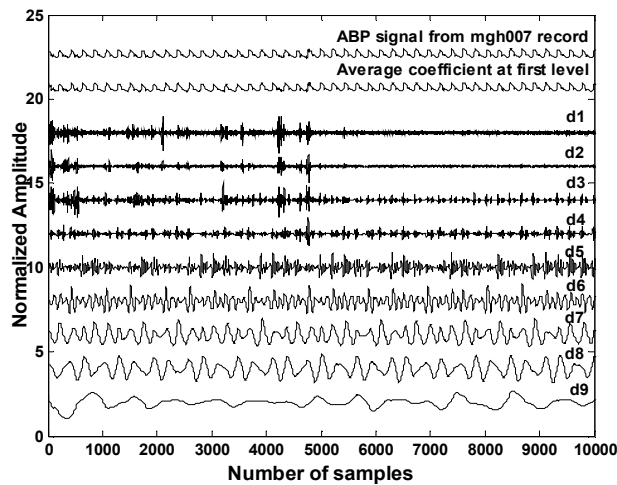


Fig 3. Wavelet decompositio structure of mgh001 using db4 wavelet

analysis [27]. There are several wavelet families like Harr, Daubechies, Biorthogonal, Coiflets, Symlets, Morlet, Mexican Hat, Meyer etc. and several other Real and Complex wavelets. However, Symlets (sym4) and Daubechies (db4) family of wavelets have been found to give details more accurately than others. Wavelet function (ψ) of sym4 and db4 wavelets are shown in figure 2(a) & 2(b) respectively.

b) Wavelet Analysis.

The selected signal under test by is decomposed up to the desired level depending upon dominant frequency components in the signal. The maximum number of decomposition levels depends upon the total number of samples present in the signal. The relationship can be expressed as-

$$2^n = N$$

Where, n = total number of levels of decomposition,
 N = total number of samples in the signal to be expressed as power of 2 for full decomposition of the signal. The ABP signal under test is decomposed up to 9 levels using db4 wavelet is shown in figure 3.

c) Selection of Detail Coefficient

The choice of selecting the required detail coefficients from the wavelet decomposition structure is dependent on the fact that the required information for feature extraction of signal is available in the detail coefficients of that signal. Therefore, the detail coefficient is selected on the basis of three types of analysis as illustrated below –

i. Energy Analysis. Maximum energy of an ABP signal is available in its higher amplitude and wider systolic complex. Other segments of the signal such as onset and dicrotic notch possess lower energy. The energy analysis of all decomposed details of ABP signal is performed. It is observed that d7 signal possesses highest energy in record mgh007 and d6 has maximum energy in abp1 signal of CSL database as shown in table II. It is observed from table II that the sum of energy of all detail coefficients and remaining one average coefficient is equal to the energy of ABP signal under test. Therefore, this energy analysis of decomposition structure proves the energy conservation principle of wavelet transform. It means that original signal can be faithfully reproduced from the

TABLE II. ENERGY CONTENTS OF DETAIL AND AVERAGE COEFFICIENTS

Signal	Detail Coefficients	Energy contents Using sym4	Energy contents Using db4
mgh007	d1	0.0000	0.0000
	d2	0.0001	0.0001
	d3	0.0025	0.0023
	d4	0.0405	0.0377
	d5	0.2521	0.2505
	d6	1.0197	1.0019
	d7	2.5670	2.5178
	d8	0.9724	0.9523
	d9	0.0212	0.0184
abp1	a9	95.1246	95.2190
	d1	0.0001	0.0001
	d2	0.0018	0.0018
	d3	0.0901	0.0870
	d4	0.9122	0.9260
	d5	2.1670	2.1364
	d6	2.3076	2.3362
	d7	0.1158	0.1026
	d8	0.1398	0.1604
d9	0.1127	0.0984	
a9	94.1528	94.1512	

decomposed components and the information in the original signal is distributed at different scales but remain preserved during decomposition.

ii. Frequency Analysis Another justification of selecting d7 for mgh007 and d6 for abp1 is its available frequency components correlated with that of ABP signal. In pressure signals, most of the signal power is in the frequency range of 0.7-3.5 Hz in humans [14]. Therefore, the Fourier analysis of ABP signal and all its decomposed detail signals is computed as shown in figure 4. From figure 4, it is observed that required frequency components lie in the in the range d6 & d7 for ABP signal of mgh007. Also it is also observed that the

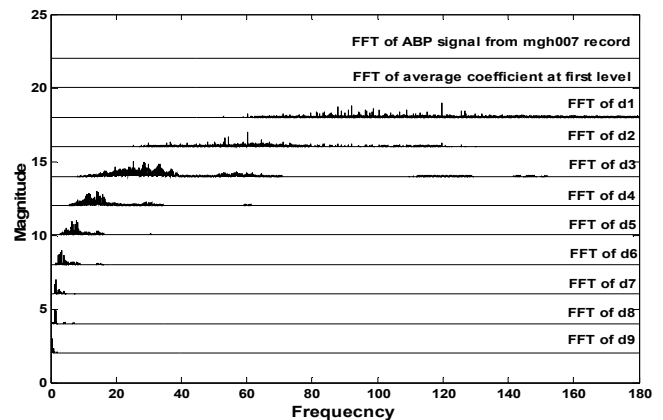


Fig 4. Frequency Analysis of detail coefficients of mgh007 signal using db4 wavelet

TABLE III. FREQUENCY CONTENTS OF DETAIL COEFFICIENTS

Signal	Detail Coefficients	Frequency content (Hz) using sym4	Frequency content (Hz) using db4
mgh007	d6	0.6467-9.01	0.6967-8.997
	d7	0.3667 – 4.52	0.8433-4.567
abp1	d5	0.6439-6.079	0.5789-6.131
	d6	0.3147-2.896	0.2783-2.943

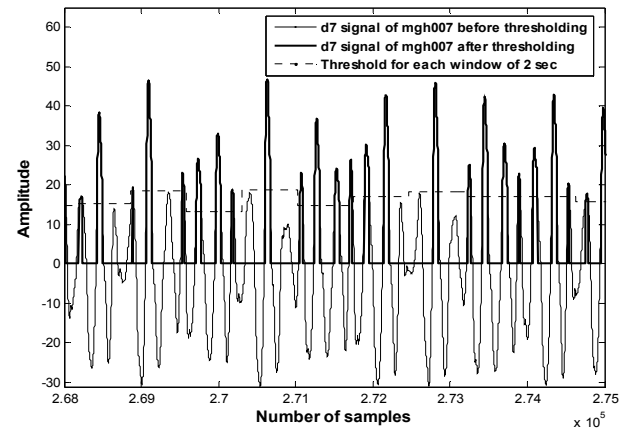
required frequency components are available between d5 and d6 for abp1 signal. Frequency range of d6 & d7 for mgh007 and d5 & d6 for abp1 is shown in table III.

iii. Cross-correlation Analysis In addition to above two analyses, cross-correlation analysis of detail coefficients individually with the original ABP signal is also performed. The results of cross-correlation analysis of detail signals with ABP signal under test are given in table IV. It is observed that the value of cross-correlation coefficient increases for d1 to d7 for mgh007 and then decreases. In case of abp1 signal, the value of cross-correlation coefficient increases for d1 to d6 and then decreases. This fact is observed while wavelet decomposition is followed using both sym4 and db4 wavelets in mgh007 and abp1 signals.

From table IV, it is evident that d7 for mgh007 and d6 of abp1 are highly correlated with the original ABP signals in time domain. The results from the above mentioned three analyses show that d7 for mgh007 and d6 in abp1 signal carries maximum information in regard to the ABP signals under test. But practically, it is seen that selecting only a particular detail signal for ABP peak detection causes loss of some information and the detected peaks are not exactly recovered. Also, it is clear from table III that information below 0.8433 Hz is lost as seen from FFT of d7 signal when ABP signal from mgh007 record is decomposed using db4 wavelet whereas d6 comprises of all required information using both sym4 and db4 wavelets for decomposition. Also, in case of abp1 signal from CSL database, d5 comprises of all relevant information in regard to frequency range of ABP signal whereas information above 2.896 Hz is missed in d6 using sym4 wavelet and signal information above 2.943 Hz is missed in case of d6 signal using db4 wavelet. Also, selection of more detail signals requires more computation. Therefore, selection of d6 & d7 signals for mgh007 record and d5 & d6 for abp1 signal are best suited for peak detection of ABP signal.

d) Window based thresholding

In soft thresholding, the selected detail coefficients below the predefined threshold are reduced to zero whereas the coefficients above the threshold tend toward zero. Hard thresholding method reduces the coefficients below the predefined threshold to zero whereas the coefficients above the threshold remain constant. Desmond B. Keenan [25] used hard thresholding method to remove high amplitude coefficients generated by ectopic beats from RR interval signals. Our method utilizes the hard thresholding method by selecting a particular threshold value from each signal segment. Pachauri

**Fig 5. Representation of window based thresholding****TABLE IV. CROSS-CORRELATION COEFFICIENTS**

Signal	Detail Coefficients	Cross-correlation coefficients using sym4	Cross-correlation Coefficients using db4
mgh007	d1	0.0012	0.0011
	d2	0.0042	0.0043
	d3	0.0215	0.0211
	d4	0.0871	0.0851
	d5	0.2171	0.2185
	d6	0.4371	0.4370
	d7	0.6930	0.6927
	d8	0.4253	0.4256
	d9	0.0465	0.0466
abp1	d1	0.0039	0.0039
	d2	0.0157	0.0157
	d3	0.1106	0.1088
	d4	0.3522	0.3548
	d5	0.5427	0.5388
	d6	0.5599	0.5633
	d7	0.1249	0.1174
	d8	0.1361	0.1469
	d9	0.1198	0.1123

etal [28] used this method for the peak detection of arterial blood pressure signal after transforming ABP signal into energy signal.

The selected detail coefficients are used for peaks detection. For this purpose, a lower threshold is applied to the selected detail signals to remove unrelated peaks appearing due to noise. This method of thresholding leads to adaptive thresholding. In this method of thresholding, the signal is segmented in to equal segments by defining a window of particular duration in terms of samples and a distinct value of threshold is selected from each segment of the signal. This type of thresholding strategy limits any large variation in the signal amplitude at a certain instant to a particular segment of the signal due to which the true peaks with lower amplitudes may be ignored in other segments if threshold is defined for the entire signal.

e) Maxima Detection

A new signal is generated by selecting the common points with positive amplitude values in both the selected detail signals after thresholding. In this newly generated signal, a maxima ' $d(i)$ ' is detected when the amplitude of previous and the succeeding are lower than the middle sample following condition (1) for maxima detection. It is possible that newly formed signal may comprise of two or more corresponding samples with same amplitude values because of the fact that pressure signals are more sinusoidal. So detection of maxima is difficult among three consecutive samples as mentioned above. In such cases, the algorithm looks for the third sample or next sample if it possesses lower amplitude following conditions (2) – (4). This process is repeated till a valid maxima is detected.

Conditions for valid maxima detection

- (1) if $d(i) > d(i-1) \& d(i) > d(i+1)$
- (2) if $d(i) > d(i-1) \& [d(i) : d(i+1)] = d(i) \& d(i+2) < d(i)$
- (3) if $d(i) > d(i-1) \& [d(i) : d(i+2)] = d(i) \& d(i+3) < d(i)$
- (4) if $d(i) > d(i-1) \& [d(i) : d(i+(n-1))] = d(i) \& d(i+n) < d(i)$

f) Peak Positions

The numbers of detected maxima are assumed as possible systolic peaks and their positions in the original ABP signal are considered as possible systolic peaks positions. As no two consecutive beats can occur before 200 ms, an interval threshold of 200 ms is applied after detection of first peak in the signal that gives rise actual number of peaks and their positions in the ABP signal under test [29].

B. Onset and Dicrotic Notch Detection

After the detection of peaks of arterial blood pressure waveform, the delineator looks for the detection of remaining features such as onset, dicrotic notch and dicrotic peak in the ABP signal. For this purpose, average coefficient at first level is found suitable. The detected peaks positions serve as the reference for detection of remaining features of signal. As discussed earlier, wavelet decomposition of the signal using the selected wavelet at first level results in detail coefficient and average coefficient. The average coefficient obtained after wavelet analysis at first level is shown in figure 3 along with detail coefficients. This approximation coefficient comprises of entire information of ABP signal and the shape of ABP signal is also retained. The analysis of this average (approximation) coefficient has been found suitable for extracting the remaining features of ABP signal. The onset positions of ABP waveform are determined after eliminating the redundant minima obtained from average coefficient after thresholding. For this purpose, detected peaks positions in the same ABP signal are taken into account. The average coefficient at first level undergoes window based amplitude thresholding by defining a window of 2 seconds. After thresholding, all the minima ' $a(i)$ ' in the signal are detected if the previous and subsequent sample in the signal have higher amplitude than the sample amplitude between them. Mathematically, the condition can be expressed as –

$$\text{if } a(i) < a(i-1) \& a(i) < a(i+1)$$

where ' a ' is the signal obtained after the approximation

coefficient at first level undergoes window based thresholding. Out of all these detected minima, only those minima are taken into account which appear after the detected peaks. If several minima are detected after the peaks positions, the minima with the minimum amplitude is registered as ABP onset.

The detected peaks and onset positions in the ABP signal are now used to detect the dicrotic notch in ABP signal. The dicrotic notch is found between the peaks and onsets in the ABP signal. For this purpose, the algorithm looks for the minima between detected peaks and onset locations. If there are several minima found between a particular peak and onset, the delineator takes into account the minima with maximum amplitude and register the minima as dicrotic notch.

B. Detection of Dicrotic Peak

The dicrotic peak appears as a peak with weak amplitude between the dicrotic notch and onset of next ABP pulse. It is the result of reflected waves from the lower extremities and the aorta. For the detection of dicrotic peak, the delineator takes into account the detected onset and dicrotic notch positions. All the maxima in the average signal at first level are determined. The maxima with maximum amplitude appearing between dicrotic notch and onset of next ABP pulse are registered as dicrotic peaks.

IV. RESULT AND VALIDATION

The algorithm has been evaluated with respect to our manual annotations on one minute segments of twenty two signals from MGH/MF waveform database, first minute segments of fourteen signals of Fantasia database, first minute segments of fifteen signals of MIT-BIH polysmographic database and first fifty thousand samples of abp1 signal of CSL database. CSL database is chosen because of the fact that it comprises of expert annotations for both the ABP signals. This database consists of annotations from two experts and also annotations from author are available [14]. This type of openly available database can help the researchers to validate their algorithms but ABP signals only from two patients may not be sufficient to have different artifacts and pathophysiological complexity of ABP waveform. Secondly, expert annotations only for peaks of ABP signals are available for both the recordings in CSL database whereas annotations for other features are not reported. The remaining three databases have ABP signals along with synchronously sampled ECG recordings. ECG signals in these databases are annotated by experts but ABP signals are not annotated so far in any of these databases. For example, simultaneous recordings for ECG signals from three leads (lead I, lead II and lead V) and ABP signals along with other signals are available in MGH/MF waveform database for each record. Also the database comprise of the expert annotations for ECG recordings.

ECG signals in MGH/MF database are available throughout the duration whereas pressure signals at certain extent are absent. Therefore same data segment of the ABP signal is selected for the analysis for which both ECG and ABP signals are available. The ECG waveform has been annotated on MGH/MF database by experts and annotation codes are

available in *ecgcodec.h*. The required codes for different beats are selected and number of beats in each ECG signal is determined for the duration when both ECG and ABP signals are available.

It has been observed that any abnormality in ECG recording is also available in ABP waveform such as in case of premature contraction, QRS complex in ECG waveform is wider than other QRS complexes whereas same abnormality in ABP waveform is observed when systolic pressure falls after the occurrence of this beat [4]. Therefore, approved ECG annotations can help to evaluate the performance of the detector. This type of validation strategy is adopted by Zong et al [13] for validation of their algorithm for onsets of ABP waveform. However, it is observed practically that although recorded simultaneously, sometimes ECG annotations do not correspond to effective ABP waveforms and number of beats between both ABP and corresponding ECG differs as shown in table V and table VI respectively. There is 23 beats difference between manual annotations of ABP peaks and ECG annotations from MGH/MF database whereas both the waveforms are clear. Sometimes 2-3 beat difference is observed between manual annotations and ECG annotations for a particular record and sometimes there is no difference between number of beats both signals. Also, ECG annotations can only give the idea about the number of peaks in ABP waveform whereas positions of peaks are to be validated manually. ECG annotations from MGH/MF database along with our manual annotations for ABP peaks for similar duration of record mgh029 is shown in fig 6. The selected data segment has 99 ECG annotations whereas 98 manual annotations for ABP peaks are observed. This anomaly is also observed in fantasia and MIT-BIH polysmographic database signals as shown in table V and table VI respectively. Therefore the delineator performance is judged by manual annotations for all four database signals. We have chosen those signal segments in which all the four signal components could be validated manually. Out of first thirty five records of MGH/MF waveform database only twenty two records were found suitable for manually annotating all four signal components. Therefore, out of first thirty five signals of MGH/MF database, mgh001, mgh003, mgh004, mgh005, mgh011, mgh013, mgh017, mgh019, mgh020, mgh021, mgh022, mgh023 and mgh024 are not included in performance evaluation of the algorithm. The problem in manually annotating all the signal components in ABP signal is mainly with the dicrotic notch and dicrotic peak positions. In Fantasia database out of total twenty signals, only fourteen signals are found suitable for manual annotation. ABP signals from records f2o01, f2o02, f2o06, f2o07, f2y03 and f2y09 of Fantasia database are not included in our manual annotations. In f2o01, f2o02 and f2o06, dicrotic notch positions are clear but dicrotic peak positions could not validated manually. In f2o07 and f2y03, there are two dicrotic notches and two dicrotic peaks for each ABP cycle and it is difficult to establish which is actual dicrotic notch and dicrotic peak whereas in f2y09, both dicrotic notch and dicrotic peak positions are not clear. In Polysmographic database, out of total eighteen signals, three signals, slp37, slp48 and slp59 are

not included in our manual annotations. In these signals also the dicrotic notch and dicrotic peaks positions are difficult to determine at various locations. Also in case of CSL database, all the four signal components were found in first fifty thousand samples in abp1 signal. Dicrotic notch and dicrotic peak positions could not be located manually in abp2 signal.

Accuracy is the most important parameter to establish the overall performance of the detector. Accuracy (A) of the detector is given by the following relation [30]

$$A = \left(1 - \frac{Ne}{Nb}\right) \times 100 \quad (iii)$$

Where 'Ne' and 'Nb' represent the total number of detection errors and annotations available in the file.

In addition to accuracy, three other measures of detector's performance i.e. sensitivity (*Se*), positive predictivity (*PP*) and error were also determined [26].

The sensitivity (*Se*), positive predictivity (*PP*), and error [15] of detector is given by the following relation

$$Se = \frac{TP}{TP + FN} \times 100 \quad (iv)$$

$$PP = \frac{TP}{TP + FP} \times 100 \quad (v)$$

$$error = \frac{(FP + FN)}{(TP + FP)} \times 100 \quad (vi)$$

Where *TP* stands for the number of true positives, *FN* and *FP* denote the number of false negatives and the false positives. True positives are the beats those have been detected correctly. False positives are the beats which are detected as beats but actually do not exist. False negatives are the beats that are missed by the detector. The sensitivity depicts the percentage of true beats to overall beats those were correctly detected by the algorithm. The positive predictivity states the percentage of true beat detections to overall annotations. The detected four signal components for one signal each for all the four databases are shown in figure 7-10. Fig 8. Also shows M Aboy and expert 1 annotations for peaks along with detector annotations for the four signal components. Overall performance of the algorithm on all the four database signals using db4 and sym4 wavelet is summarized in table V and table VI respectively. It is clear from the table V and table VI that analysis with db4 wavelet results in more false detections for all the four components of ABP signal as compared to sym4 wavelet as a result reducing positive predictivity for MGH/MF and fantasia database signals. In terms of sensitivity, results by both the wavelets on both databases are comparable. On the contrary, performance of db4 wavelet is better on MIT-BIH polysmographic database signal in comparison to sym4 wavelet. for all four parameters of performance evaluation such as accuracy, sensitivity, positive predictivity and error analysis of the delineator. Performance of both the wavelets is similar on CSL database signals.

V. CONCLUSION AND DISCUSSION

An algorithm for delineation of arterial blood pressure waveform is proposed. The algorithm utilizes wavelet

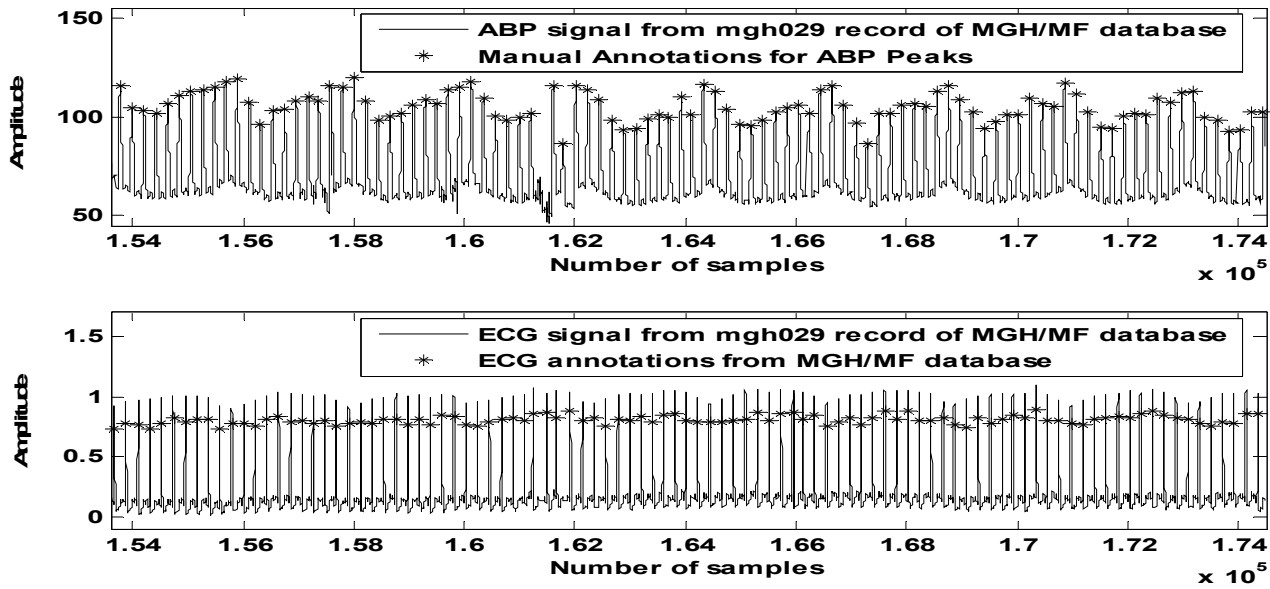


Fig 6. Manual annotations for ABP signal and ECG annotations from MGH/MF database for mgh029 record ((153601: 174500))

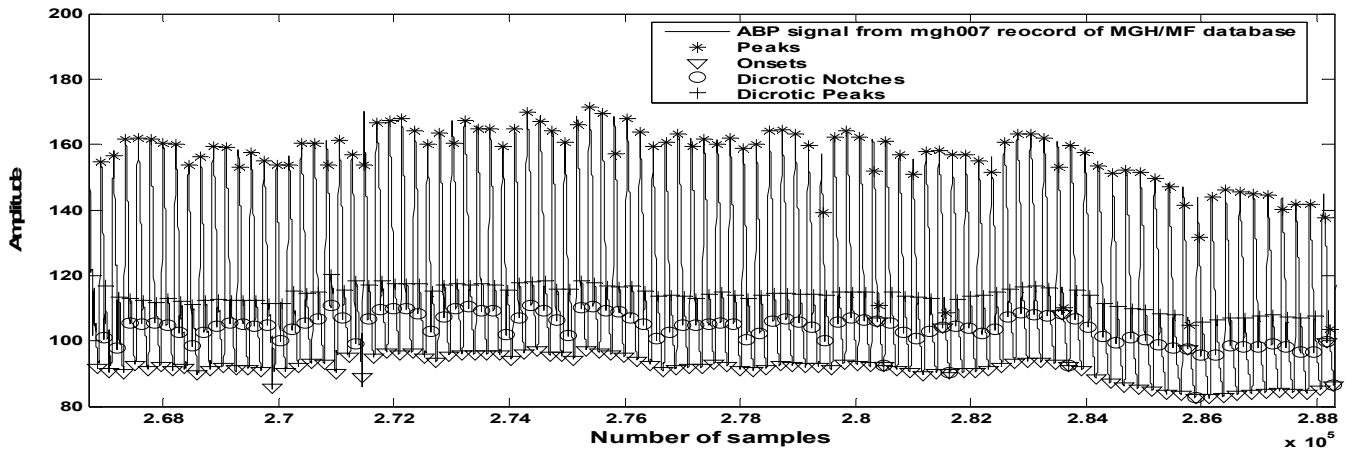


Fig 7. Detected Peaks, onsets, dicrotic notch and dicrotic peaks in ABP signal of mgh007 (266701:288300) record of MGH/MF waveform database

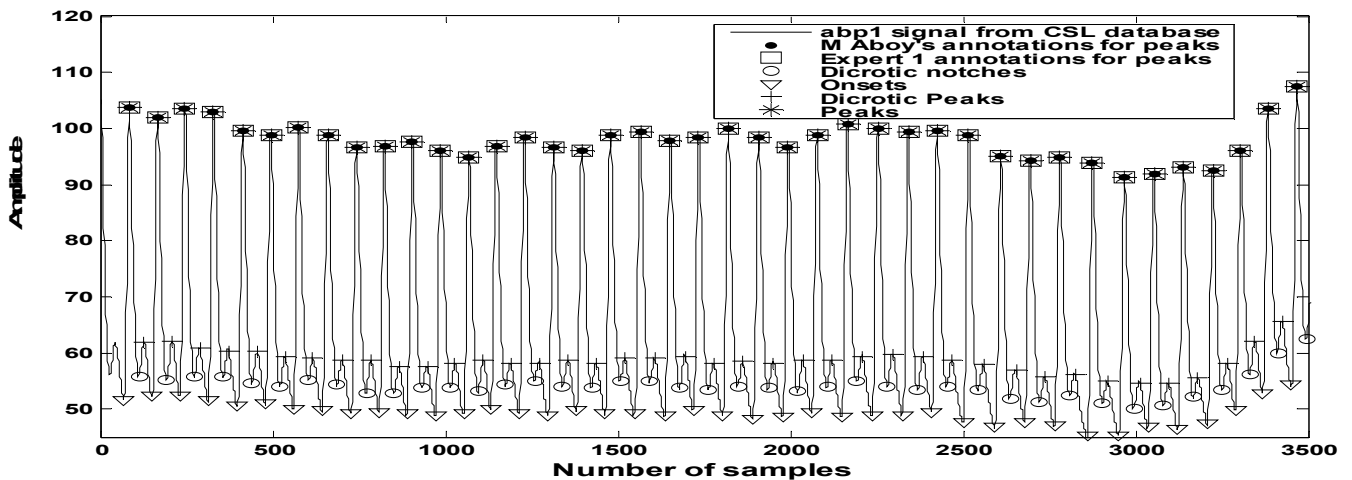


Fig 8. Detected Peaks, onsets, dicrotic notch and dicrotic peaks in abp1 signal of CSL database

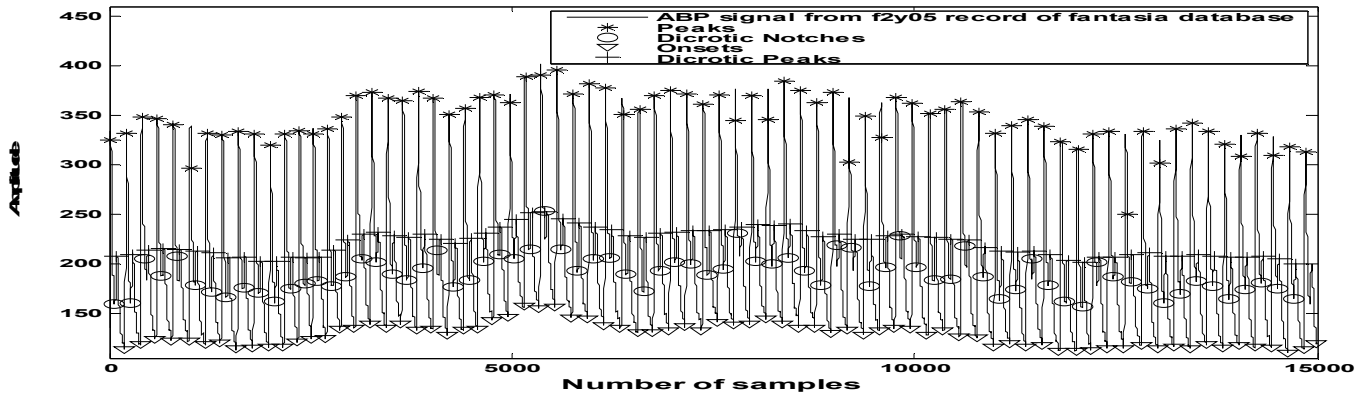


Fig 9. Detected Peaks, onsets, dicrotic notch and dicrotic peaks in ABP signal (first one minute segment (1:15000) samples) of f2y05 record of Fantasia database

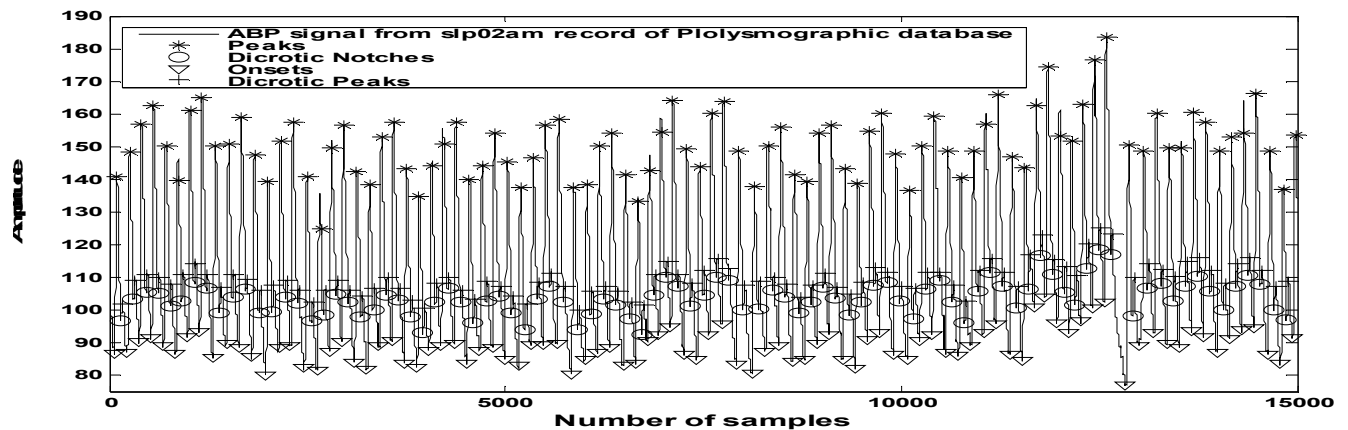


Fig 10. Detected Peaks, onsets, dicrotic notch and dicrotic peaks in ABP signal (first one minute segment (1:50000) samples) of slp02am record of MIT-BIH Polysmographic database

TABLE V. OVERALL PERFORMANCE OF THE DELINEATOR WITH Db4 WAVELET

Database	Features	ECG annotations		Manual Annotations	Total Detector Annotations	TP	FN	FP	A (%)	Se (%)	PP (%)	Error (%)
MGH/MF (22 Signals)	PK	1896		1873	1941	1862	03	93	94.87	99.83	95.24	4.9
	OS			1868	1951	1858	03	112	93.84	99.83	94.31	5.8
	DN			1860	1919	1843	06	87	95.00	99.67	95.49	4.8
	DP			1860	1839	1810	31	50	95.64	98.31	97.31	4.35
Fantasia (14 Signals)	PK	949		884	912	879	05	33	95.70	99.43	96.38	4.1
	OS			889	921	884	05	36	95.38	99.43	96.08	4.45
	DN			881	870	845	36	25	93.07	95.91	97.12	6.9
	DP			881	859	836	18	18	95.91	97.89	97.89	4.21
MIT-BIH Polysmographic (15 Signals)	PK	1101		1110	1097	1093	17	04	98.10	98.46	99.63	1.91
	OS			1110	1099	1094	16	05	98.10	98.55	99.54	1.91
	DN			1096	1052	1049	47	03	99.53	95.71	99.71	4.75
	DP			1096	1060	1044	52	16	93.79	95.25	98.49	6.41
CSL (01 Signal) (1:50000) samples	PK	M Aboy	Expert	602	602	602	-	-	100	100	100	0.00
	OS			602	602	602	-	-	100	100	100	0.00
	DN			602	602	600	01	01	99.67	99.84	99.84	0.34
	DP			601	601	600	01	01	99.67	99.84	99.84	0.34

PK - Peaks, OS - Onsets, DN - Dicrotic notches, DP – Dicrotic Peaks

TABLE VI. OVERALL PERFORMANCE OF THE DELINEATOR WITH Sym4 WAVELET

Database	Features	ECG annotations		Manual Annotations	Detector Annotations	TP	FN	FP	A (%)	Se (%)	PP (%)	Error (%)
MGH/MF (22 Signals)	PK	1896		1873	1887	1866	09	42	97.27	99.52	97.79	2.67
	OS			1868	1896	1862	07	31	97.96	99.62	98.36	2.007
	DN			1860	1864	1848	12	15	98.54	99.35	99.19	1.449
	DP			1860	1820	1818	36	09	97.58	98.05	99.50	2.46
Fantasia (14 Signals)	PK	949		884	876	864	18	14	96.38	97.95	98.40	3.64
	OS			889	885	872	16	13	96.73	98.19	98.53	3.27
	DN			881	862	853	25	12	96.93	97.15	98.61	3.12
	DP			881	842	841	33	06	95.57	96.23	99.29	4.6
MIT-BIH Polysomographic (15 Signals)	PK	1101		1110	1091	1083	27	08	96.84	97.56	97.56	3.2
	OS			1110	1095	1090	20	05	97.74	98.19	99.54	2.28
	DN			1096	1076	1071	24	05	97.35	97.80	99.53	2.69
	DP			1096	1071	1066	29	05	96.89	97.35	99.53	3.17
CSL (01 Signal) (1:50000) samples	PK	M Aboy	Expert	602	602	602	-	-	100	100	100	0.00
	OS			602	602	602	-	-	100	100	100	0.00
	DN	602	602	601	601	600	01	01	99.67	99.84	99.84	0.34
	DP			601	601	600	01	01	99.67	99.84	99.84	0.34

transform to decompose the signal under test at each scale. The algorithm is robust against physiological interferences and varying amplitudes of the signal on time scale. The performance of the algorithm is judged considering the signals from four databases. Implementation of wavelet based technique for feature extraction of ABP signals shows the capability of wavelet transform in biomedical signal processing. Wavelet based method has been used by Sahambi et al [29] for ECG feature extraction. So far most of the methods used for validation of pressure beat detection algorithms are based on proprietary datasets those were acquired from experimental animals [31] and limited to few beats or patients only [32]. The assessment of beat detection algorithms on those proprietary databases is not possible. Validation of algorithm on the signals of open access MGH/MF waveform database, Fantasia database, MIT-BIH polysomographic database and CSL database opens a pathway to generalize the algorithm. Consequently, this may result to describe the cardiac functions more accurately while combining with ECG algorithms. Assessment of the algorithm on ABP signals from different database with different subjects adds to the robustness of the method as signals on these databases encompass various artifacts, instrumental errors and physiological complexities. The proposed algorithm can be employed to detect myocardial ischemia, detection of premature ventricular contraction (PVC) and premature supra-ventricular contraction (PSC) beats along with ECG signal to enhance the accuracy of disease identification. The proposed algorithm can also be employed for cardiac output monitoring [2], estimating pressure pulse index [3] and in the evaluation of arterial stiffness [6]. Also, use of ABP waveform analysis has been observed with ECG signal to reduce the false alarms

in case of critical arrhythmias [9]. Our aim in this paper is mainly to check the performance of the algorithm with ABP signals of subjects of different age groups, sex that could combine the signals of various pathological complexities

rather than a larger signal segment with one subject. Although the developed algorithm is applicable for the signals with long duration without any significant computation time yet performance evaluation with one minute segment is shown due to the problem of manually annotating the large signal segments.

REFERENCES

- [1] Miyakawa K, Koepfen HP, Polosa C., "Mechanism of Blood Pressure wave", Japan Scientific Press, Springer-Verlag, Tokyo, 1984.
- [2] JX Sun, AT Reiser, M Saeed, RG mark, "Estimating Cardiac Output from Arterial Blood Pressure waveforms: A Critical Evaluation using the MIMIC II Database", www.physionet.org/physiotools/cardiac-output/doc/s54-5.pdf.
- [3] Mateo Aboy, James McNames, Tran Thong, Charles R. Phillips, Miles S. Ellenby, and Brahm Goldstein, "A Novel Algorithm to Estimate the Pulse Pressure Variation Index", IEEE Transactions on Biomedical Engineering, Vol. 51, NO. 12, December 2004, IEEE
- [4] Ramaswamy, Palaniappan, Shankar M. Krishnan, "Detection of Ectopic Heart Beats using ECG and Blood Pressure Signals", International Conference on Signal Processing & Communications (SPCOM), 2004
- [5] J.N. Cohn, S. Finkelstein, G. McVeigh, D. Morgan, L. LeMay, J. Robinson, J. Mock, "Noninvasive pulse wave analysis for the early detection of vascular disease," Hypertension 26 (1995) 503-508.
- [6] E.R. Rietzschel, E. Boeykens, M.L.D. Buyzere, D.A. Duprez, D.L. Clement, "A comparison between systolic and diastolic pulse contour analysis in the evaluation of arterial stiffness," Hypertension 37 (2001) e15-e22.
- [7] J.I. Davies, A.D. Struthers, "Beyond blood pressure: pulse wave analysis—a better way of assessing cardiovascular risks," Future Cardiology 1 (2004) 69-78.
- [8] A. de Sa Ferreira, J.B. Filho, I. Cordovil, M.N. de Souza, "Three-section transmission line arterial model for noninvasive assessment of vascular remodeling in primary hypertension," Biomedical Signal Processing and Control 4 (1) (2009) 2-6.
- [9] Aboukhalil A, Nielsen L, Saeed M, Mark RG, Clifford GD, "Reducing false alarm rates for critical arrhythmias using the arterial blood pressure waveform," Journal of Biomed Informatics, Vol 41 Issue 3, June 2008 442-451.
- [10] Michael A. Navakatikyan, Carolyn J. Barrett, Geoffrey A. Head, James H. Ricketts and Simon C. Malpas, "A Real-Time Algorithm for the Quantification of Blood Pressure Waveforms", IEEE Transactions on Biomedical Engineering, Vol. 49, No. 7, July 2002

- [11] W Zong, GB Moody, RG Mark, “Effects of Vasoactive Drugs on the Relationship between ECG-Pulse Wave Delay Time and arterial Blood Pressure in ICU Patients”, *Computers in Cardiology* 1998 Vol. 25, PP 673-676.
- [12] M. Aboy, C. Crespo, J. McNames, B. Goldstein, “Automatic Detection Algorithm for Physiologic Pressure Signal Components”, *Proceedings of Second Joint EMBS/BMES Conference Houston, TX USA, OCT 23-26, 2002*
- [13] W Zong, T Heldt, GB Moody, RG Mark, “An Open Source Algorithm to Detect Onset of Arterial waveform Pulses”, *Computers in Cardiology*, 2003; 30:259-262,
- [14] Mateo Aboy, James Mc Names, Daniel Tsunami, Miles S. Ellenby, and Brahm Goldstein, “An Automatic Beat Detection Algorithm for Pressure Signals”, *IEEE Transactions on Biomedical Engineering*, Vol. 52, No. 10, October 2005.
- [15] Bing Nan Li, Ming Chui Dong, Mang I. Vai, “On an automatic delineator for arterial blood pressure waveforms”, *Biomedical Signal Processing and Control* 5 (2010) 76–81
- [16] S.A.A.P. Hocksel, J.R.C. Jansen, J.A. Blom, Schruder, “Detection of Dicrotic Notch in Arterial Pressure Signals”, *Journal of Clinical Monitoring* 13: 309-316, 1997
- [17] <http://www.physionet.org/mghdb>
- [18] <http://www.physionet.org/physiobank/database/fantasia>
- [19] <http://www.physionet.org/physiobank/database/slpdb>
- [20] <http://bsp.pdx.edu>
- [21] Daubechies, I. and Sweldens, W., “Factoring Wavelet Transforms into Lifting Steps”, Preprint, Bell Laboratories, Lucent Technologies (1996).
- [22] R. G. Hohlfeld, C. Rajagopalan, and G. W. Neffl “Wavelet Signal Processing of Physiologic Waveforms,” Wavelet Technologies, Inc., Copyright 2004
- [23] S. Mallat and S. Zhong, “Characterization of signals from multiscale edges,” *IEEE Trans. Pattern Anal. Mach. Intell.* 1992, **14** 710–32
- [24] Fayyaz-ul-Amir Afsar Minhas and Muhammad Arif, “Robust electrocardiogram (ECG) beat classification using discrete wavelet transform,” *Physiol. Meas.* 29 (2008) 555–570
- [25] Desmond B. Keenan, “Detection and Correction of Ectopic Beats for HRV Analysis Applying Discrete Wavelet Transforms,” *International Journal of Information Technology* Volume 2 Number 1.
- [26] (1998) ANSI/AAMI CE57: Testing and Reporting Performance Results of Cardiac Rhythm and ST Segment Measurement Algorithms. (AAMI) Recommended Practice/American National Standard. [Online]. Available: <http://www.aami.org>
- [27] S. Z. Mahmoodabadi, A. Ahmadian, M. D. Abolhasani, M. Eslami, J. H. Bidgoli, “ECG Feature Extraction Based on Multiresolution Wavelet Transform,” *Proceedings of the 2005 IEEE, Engineering in Medicine and Biology 27th Annual Conference Shanghai, China, September 1-4, 2005.*
- [28] Awadhesh Pachauri and Manabendra Bhuyan, “ABP Peak Detection Using Energy Analysis Technique,” *International Conference on Multimedia, Signal Processing and Communication Technologies (IMPACT) - 2011*, page no.36-39, IEEE explore and digital library.
- [29] S.Sahambi, S.N. Tandon, R.K.P. Bhatt, “Using Wavelet Transforms for ECG Characterization, An Online Digital Signal Processing System,” *IEEE Engineering In Medicine & Biology*, Jan/Feb, 1997
- [30] Omer T. Inan, Laurent Giovangrandi, and Gregory T. A. Kovacs, “Robust Neural-Network based classification of Premature Ventricular Contractions using wavelet transform and timing interval features”, *IEEE transactions on Biomedical Engineering*, Vol. 53, No. 12, December 2006
- [31] A. Donelli, J.R.C. Jansen, B. Hoeksel, P. Pedeferra, R. Hanania, J. Bovelander, et al., “Performance of a real-time dicrotic notch detection and predication algorithm in arrhythmic human aortic pressure signals,” *Journal of Clinical Monitoring and Computing* 17 (2002) 182–185.
- [32] M.I. Oppenheim, D.F. Sittig, “An innovative dicrotic notch detection algorithm which combines rule-based logic with digital signal processing techniques,” *Computers and Biomedical Research* 28 (1995) 154–170.